

# Reconfiguring photonic metamaterials with currents and magnetic fields

João Valente,<sup>1,a)</sup> Jun-Yu Ou,<sup>1</sup> Eric Plum,<sup>1,b)</sup> Ian J. Youngs,<sup>2</sup> and Nikolay I. Zheludev<sup>1,3,c)</sup>

<sup>1</sup>*Optoelectronics Research Centre and Centre for Photonic Metamaterials, University of Southampton, Southampton SO17 1BJ, United Kingdom*

<sup>2</sup>*Physical Sciences Department, DSTL, Salisbury SP4 0JQ, United Kingdom*

<sup>3</sup>*Centre for Disruptive Photonic Technologies, Nanyang Technological University, Singapore 637378, Singapore*

(Received 29 November 2014; accepted 15 February 2015; published online 17 March 2015)

We demonstrate that spatial arrangement and optical properties of metamaterial nanostructures can be controlled dynamically using currents and magnetic fields. Mechanical deformation of metamaterial arrays is driven by both resistive heating of bimorph nanostructures and the Lorentz force that acts on charges moving in a magnetic field. With electrically controlled transmission changes of up to 50% at sub-mW power levels, our approaches offer high contrast solutions for dynamic control of metamaterial functionalities in optoelectronic devices. © 2015 AIP Publishing LLC.

[<http://dx.doi.org/10.1063/1.4913609>]

Dynamic control over metamaterial functionalities has become a major research challenge, as the numerous novel and dramatically enhanced functionalities that metamaterials can provide are usually narrow-band and fixed. The use of superconductors,<sup>1,2</sup> phase change media,<sup>3–5</sup> liquid crystals,<sup>6–9</sup> nonlinear materials,<sup>10–13</sup> graphene,<sup>14,15</sup> and coherent optical interactions<sup>16,17</sup> has been investigated to achieve metamaterial properties tunable via temperature, external fields, light intensity or phase, or carrier injection<sup>18,19</sup> (for an extended list of references, see Ref. 20). Magnetoelastic and MEMS reconfigurable metamaterials have been realized for THz and sub-THz frequencies<sup>21–26</sup> and recently, reconfigurable metamaterials operating in the optical spectral range have been demonstrated.<sup>27,28</sup> However, the latter require large ambient temperature changes or engage irreversible structural transitions to achieve significant optical contrast. Therefore, a practical solution for reversible large-range tuning of photonic metamaterial properties is still needed. Here, we demonstrate that reconfigurable photonic metamaterials controlled by electrical currents and magnetic fields provide such a practical solution for reversible large-range tuning and modulation of optical metamaterial functionalities. Our approach takes advantage of the changing balance of forces at the nanoscale, where bilayers of nanoscale thickness bend strongly in response to temperature changes and weak elastic forces allow the magnetic Lorentz force to cause substantial deformation of the picogram-scale moving parts.

Optical properties of metallic nanostructures, such as the metamaterial investigated here, are determined by the localized plasmonic response of coupled oscillations of conduction electrons and the electromagnetic near-field induced by the incident light. In this work, dynamic control over metamaterial optical properties is achieved by exploiting the strong electromagnetic interactions between the metamaterial building blocks, the metamolecules. By changing the physical arrangement of the nanoscale metamolecules, we

change their coupling and therefore the optical properties of the metamaterial array. Synchronous rearrangement of about 1000 plasmonic resonators at the nanoscale is achieved exploiting two simple physical principles: (i) bilayers consisting of materials with different thermal expansion coefficients will bend in response to temperature changes and (ii) electric charges moving in a magnetic field will be subject to the magnetic Lorentz force, see Fig. 1. Selective resistive heating of alternating bridges and thus their deformation by differential thermal expansion, as well as, selective magnetic deformation of current-carrying bridges when the nanostructure is placed in a magnetic field, will change distance and coupling between adjacent resonators, resulting in changes of the metamaterial's optical properties.

The reconfigurable nanostructure, which is shown by Fig. 2, was fabricated by focused ion beam milling from a

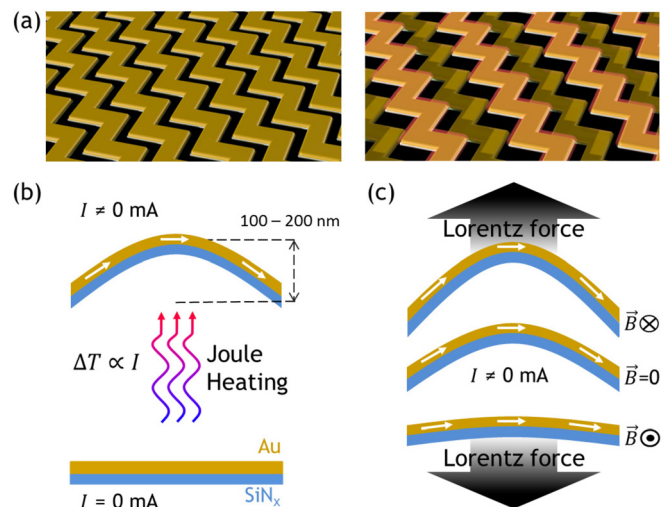


FIG. 1. Actuation mechanisms for electrically and magnetically reconfigurable metamaterial. (a) Artistic impression of the metamaterial's OFF state (left) and ON state (right). (b) Electrothermal tuning: Currents flowing in electrically connected bridges will produce Joule heating and bow the bilayered structure due to differential thermal expansion of gold (yellow) and silicon nitride (blue). (c) Magnetic tuning: Moving charges (current) in a static magnetic field will be subject to the Lorentz force that can be used to enhance or inhibit the electrothermal deformation.

<sup>a)</sup>Electronic mail: [jpv1f11@orc.soton.ac.uk](mailto:jpv1f11@orc.soton.ac.uk)

<sup>b)</sup>Electronic mail: [erp@orc.soton.ac.uk](mailto:erp@orc.soton.ac.uk)

<sup>c)</sup>Electronic mail: [niz@orc.soton.ac.uk](mailto:niz@orc.soton.ac.uk). URL: [www.nanophotonics.org.uk](http://www.nanophotonics.org.uk)

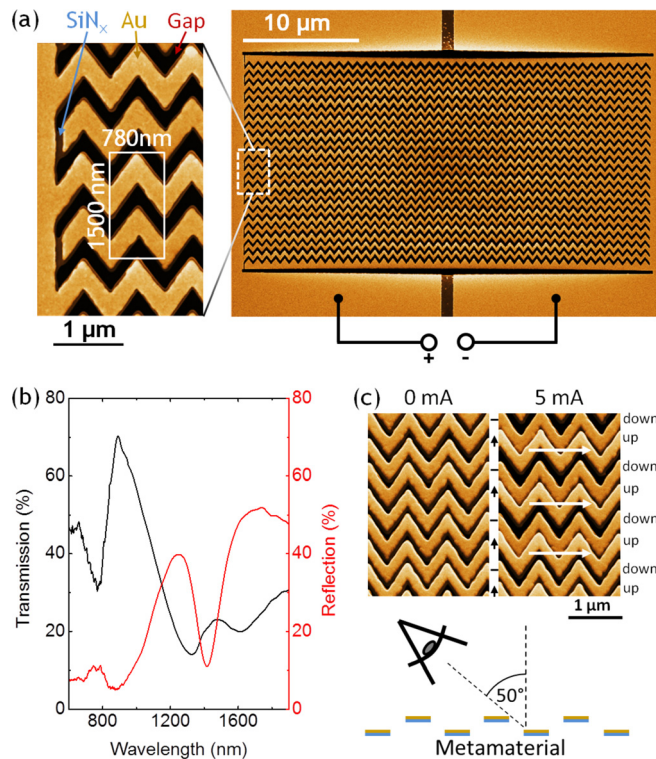


FIG. 2. Reconfigurable photonic metamaterial. (a) False color scanning electron microscope (SEM) image showing the reconfigurable photonic metamaterial. The inset shows an enlarged metamaterial section, where a metamolecule has been highlighted and the electrical connections at the bridge ends can be clearly seen. (b) Transmission and reflection reference spectra for light polarized perpendicular to the bridges of the nanostructure in the absence of currents and magnetic fields. (c) SEM images taken with 0 mA and 5 mA current applied to the metadvice. The images were taken at  $50^\circ$  from the normal (see schematic) to visualize the out-of-plane deformation of the nanostructure and current-carrying bridges are marked by white arrows.

50 nm thick low stress silicon nitride membrane covered by a 50 nm thick thermally evaporated gold layer. The overall size of the metamaterial array is  $35 \mu\text{m} \times 20 \mu\text{m}$  and its period is 780 nm along the bridges. Out-of-plane motion of every second bridge will increase the nanostructure's periodicity perpendicular to the bridges from 750 nm to 1500 nm. For the nanostructure to be an effective medium film, i.e., to transmit and reflect light without scattering, the optical wavelength shall be longer than the unit cell in all directions. Thus, strictly speaking, the deformed nanostructure is a non-diffracting metamaterial only at wavelengths longer than 1500 nm, while deformation leads to a regime of tunable diffraction at shorter wavelengths. The photonic metamaterial consists of an array of plasmonic V-shaped resonators, which give rise to optical resonances in the near-infrared, see Fig. 2(b). In order to allow movement of the nanostructure, the gold resonators are flexibly supported by silicon nitride bridges, which deform easily due to their spring-like chevron shape. Placing sub-micron scale plasmonic resonators on much longer elastic support structures allows us to realize a reconfigurable photonic metamaterial without moving parts on the size scale of a metamolecule. Changes of the inter-resonator coupling require relative movement of the bridges; therefore, every second bridge has been electrically connected to both electrical terminals at the bridge ends, see the inset to Fig. 2(a).

Application of a voltage across the device terminals leads to electrical currents and resistive heating in all 12 electrically connected bridges. Due to the large thermal expansion coefficient of gold ( $14.2 \times 10^{-6} \text{K}^{-1}$ ), which exceeds that of silicon nitride ( $2.8 \times 10^{-6} \text{K}^{-1}$ ) by a factor of 5, the electrically connected bridges bow upwards.<sup>29</sup> This is illustrated by Fig. 2(c), which shows the central part of the nanostructure with a viewing angle of  $50^\circ$  from the normal to visualize the out-of-plane deformation when currents are applied. The central portion of the current-carrying bridges is raised continuously by about 200 nm as the magnitude of the applied device current is increased to 5 mA and the bridges return to their original position when the driving current is withdrawn.

This continuous and fully reversible change in the physical arrangement of the nanostructure is accompanied by dramatic changes in the metamaterial's optical properties. For example, transmission for electromagnetic waves polarized perpendicular to the bridges increases by up to 26% in the diffracting regime around 1250 nm and decreases by up to 47% in the non-diffracting regime around 1600 nm, see Fig. 3(a). Similar continuous and reversible changes of at least 40% were observed in transmission and reflection for both eigenpolarizations. All electrothermal changes of the metamaterial's optical properties do not depend on the current direction. Optical spectra were collected from the central portion of the reconfigurable metamaterial using a microspectrophotometer.

Resistive heating, differential thermal expansion, and the resulting bridge displacement are all proportional to the

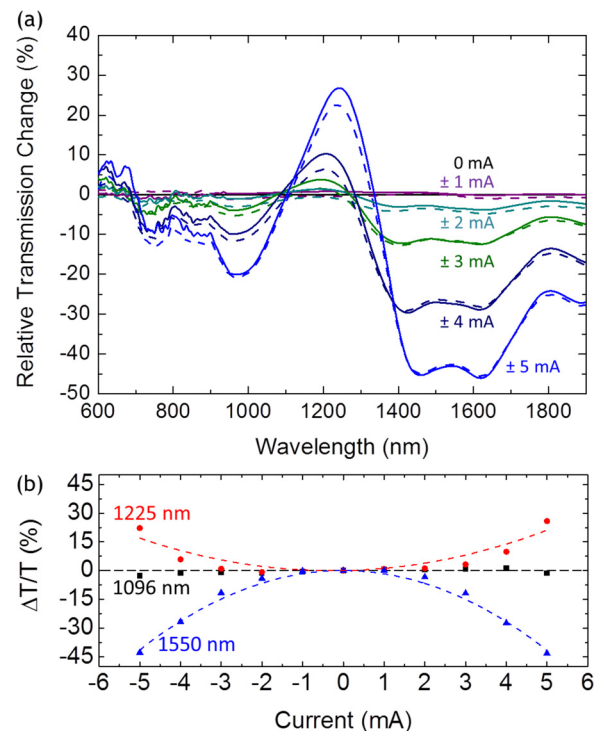


FIG. 3. Electrothermal tuning. (a) Spectral dependence of the current-induced transmission change relative to a reference case where no current is applied. The incident light is polarized perpendicular to the bridges. Positive (solid lines) and negative (dashed lines) currents lead to the same transmission change within experimental accuracy. (b) Relative transmission change as function of applied current for characteristic wavelengths, where dashed lines show parabolic fits.

power dissipation in the nanostructure, which is proportional to the square of the applied current. This quadratic current dependence of the nanostructure's physical configuration can be seen in the electrothermal changes of its optical properties, which resemble a parabola when plotted as a function of current, see Fig. 3(b). Based on the nanostructure's measured resistance of  $R = 22 \Omega$ , the device power consumption at a current of  $I = 5 \text{ mA}$  is  $RI^2 = 550 \mu\text{W}$ . Considering conductive cooling, this corresponds to an equilibrium temperature at the centre of the current-carrying bridges that is raised by about 200 K, which is consistent with the observed 200 nm bridge movement as a bridge displacement in the region of 1 nm/K is expected from beam theory.<sup>29</sup>

While electrothermal tuning of metamaterial properties offers large contrast, its response time is inherently limited by the cooling timescale of the nanostructure, which is about 10  $\mu\text{s}$  according to conductive cooling estimates. This limitation does not apply to non-thermal driving mechanisms and therefore we propose the use of the magnetic Lorentz force, which responds as quickly as applied currents or magnetic fields can be modulated.

As illustrated by Fig. 1(c), a magnetic field  $\mathbf{B}$  in the metamaterial plane and perpendicular to a bridge of length  $L$  carrying a current  $\mathbf{I}$  will lead to a Lorentz force  $\mathbf{F} = L\mathbf{I} \times \mathbf{B}$  acting perpendicular to the metamaterial plane. Depending on the mutual directions of current and magnetic field, this force can be directed upwards, increasing the electrothermal deformation, or downwards, reducing the electrothermal deformation. The manifestation of this can be clearly seen in the metamaterial's optical properties. Fig. 4 shows how the transmission of the metadvice with 4 mA applied current is changed by the magnetic field. For positive currents and magnetic fields, the Lorentz force is directed downwards, pushing the current-carrying bridges back into the metamaterial plane and comparison with Fig. 3 reveals that this largely reverses the electrothermal transmission changes discussed above. On the other hand, reversal of the direction of magnetic field (or current) reverses the Lorentz force direction such that it increases the electrothermal deformation and the associated transmission changes. The metamaterial's transmission changes continuously as a function of magnetic field, reaching magnetically induced transmission increases of more than 20% when 130 mT are applied, corresponding to a Lorentz force of about 1.5 nN per bridge and 10 s of nm bridge displacement. Magnetic modulation of the metamaterial's optical properties on the background of a constant electrothermal effect can be easily achieved with a constant static magnetic field by modulating the current direction, leading to 25% transmission modulation for  $\pm 4 \text{ mA}$  currents and 130 mT magnetic field without being limited by thermal timescales. This approach promises fast electric control of optical properties with high contrast in optoelectronic devices that include a pair of (e.g., neodymium) magnets.

The physical deformation of the nanostructure influences its optical properties by affecting inter-metamolecular coupling, strength and spectral position of associated resonances, and diffraction. In general, this leads to a complicated relationship between optical properties and bridge displacement, which may be approximated as linear for small bridge movements. The plasmonic resonators are most strongly coupled

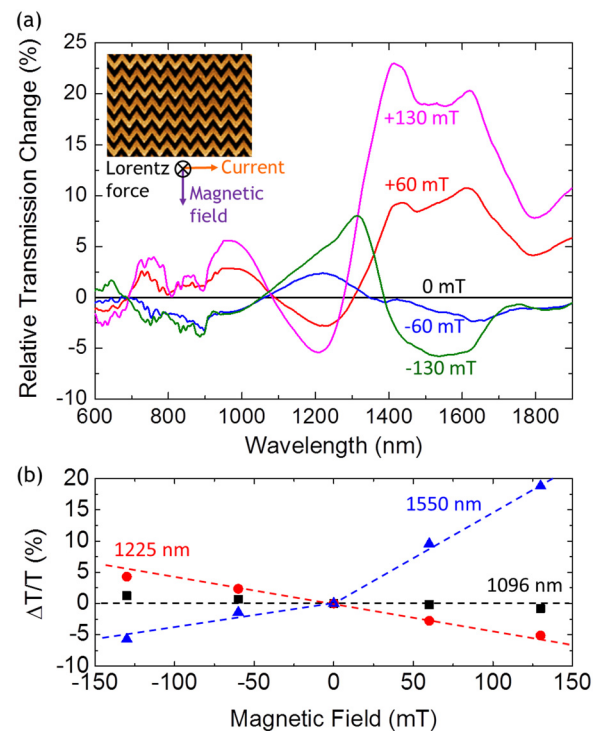


FIG. 4. Magnetic tuning. (a) Spectral dependence of the relative transmission change resulting from application of various magnetic fields to the metamaterial device, while a constant 4 mA current is applied. The applied magnetic field and the electric field of the incident wave are directed perpendicular to the plasmonic metamaterial bridges in the metamaterial plane. (b) Relative transmission change as function of applied magnetic field for characteristic wavelengths. Quasi-linear and saturation regimes are indicated by dashed lines.

when their spacing is small, leading to high sensitivity to mechanical rearrangement. Thus, a reduction of the gap between the bridges resulting from a reduction of the applied current (Fig. 3) or application of a magnetic field directed to counteract the nanostructure's electrothermal deformation (Fig. 4) leads to large changes in the metamaterial's optical properties throughout the studied spectral range. On the other hand, the metamaterial's optical properties show signs of saturation when the Lorentz force is directed to further increase the deformation (Fig. 4). The linear magnetic field dependence of the Lorentz force and the associated magnetic bridge displacement can be seen in the nanostructure's optical properties below the saturation regime, see Fig. 4(b).

Of course, electrothermal and magnetic control of reconfigurable metamaterials is not limited to gold chevron resonators, but it can in principle be applied to any array of metamolecules that can be supported by a set of bridges. This way, tunability can be added to metamaterial arrays with all sorts of useful functionalities. Where the metamolecules themselves do not provide a continuous electrical path, an additional layer of an electrically conductive material such as a transparent conductive oxide can be added and in case of electrothermal control an asymmetric layering of materials with substantially different thermal expansion coefficients needs to be chosen to ensure that resistive heating will lead to structural deformation.

In general, the achievable modulation amplitude is controlled by the mechanical, electrical, and optical properties



of the nanostructure, applied electrical currents and magnetic fields. Both the electrothermal and magnetic displacements and thus modulation amplitudes may be increased by using longer bridges manufactured from a more elastic membrane. Larger modulation can also be achieved by increasing the sensitivity of the metamaterial's optical properties to nanoscale displacements through reduced spacing of metamolecules that are optimized to be strongly coupled. Larger magnetic tuning may be achieved by increasing both magnetic fields and electrical currents, resulting in a larger Lorentz force. In particular, higher quality gold films (e.g., single crystal films) would allow both higher currents and lower operating temperatures by reducing resistive heating.

In summary, we demonstrate practical solutions for large-range tuning of reconfigurable photonic metamaterials: (i) electrothermal tuning exploiting local resistive heating and differential thermal expansion to reconfigure the nanostructure and (ii) magnetic modulation exploiting the Lorentz force on current-carrying reconfigurable parts of the metamaterial which is placed in an external magnetic field. Electrothermal tuning delivers optical contrast on the order of 50% and promises 10  $\mu$ s response times, while magnetic tuning offers 25% optical contrast without being limited by thermal timescales. In addition, <1 mW power consumption and few-mA control currents make electrothermally and magnetically reconfigurable metamaterials operating in an ambient temperature environment and without special intensity requirements a practical solution for real tunable meta-devices for the optical part of the spectrum. Potential applications stretch from tunable filters and programmable transformation optics devices to dynamic control of metamaterial functionalities and manipulation of light.

This work was supported by the UK's Defence Science and Technology Laboratory (Grant No. DSTLX1000064081), the U.S. Office of Naval Research (Grant No. N000141110474), the MOE Singapore (Grant No. MOE2011-T3-1-005), the Leverhulme Trust, the Royal Society, and the UK's Engineering and Physical Sciences Research Council through the Nanostructured Photonic Metamaterials Programme Grant.

<sup>1</sup>M. Ricci, N. Orloff, and S. M. Anlage, *Appl. Phys. Lett.* **87**, 034102 (2005).

<sup>2</sup>V. Savinov, V. A. Fedotov, S. M. Anlage, P. A. J. de Groot, and N. I. Zheludev, *Phys. Rev. Lett.* **109**, 243904 (2012).

<sup>3</sup>T. Driscoll, H. T. Kim, B. G. Chae, B. J. Kim, Y. W. Lee, N. M. Jokerst, S. Palit, D. R. Smith, M. D. Ventra, and D. N. Basov, *Science* **325**, 1518 (2009).

- <sup>4</sup>M. J. Dicken, K. Aydin, I. M. Pryce, L. A. Sweatlock, E. M. Boyd, S. Walavalkar, J. Ma, and H. A. Atwater, *Opt. Express* **17**, 18330 (2009).
- <sup>5</sup>Z. L. Sámsón, K. F. MacDonald, F. D. Angelis, B. Gholipour, K. Knight, C.-C. Huang, E. D. Fabrizio, D. W. Hewak, and N. I. Zheludev, *Appl. Phys. Lett.* **96**, 143105 (2010).
- <sup>6</sup>Q. Zhao, L. Kang, B. Du, B. Li, J. Zhou, H. Tang, X. Liang, and B. Zhang, *Appl. Phys. Lett.* **90**, 011112 (2007).
- <sup>7</sup>D. H. Werner, D.-H. Kwon, I.-C. Khoo, A. V. Kildishev, and V. M. Shalaev, *Opt. Express* **15**, 3342 (2007).
- <sup>8</sup>A. Minovich, J. Farnell, D. N. Neshev, I. McKerracher, F. Karouta, J. Tian, D. A. Powell, I. V. Shadrivov, H. H. Tan, C. Jagadish *et al.*, *Appl. Phys. Lett.* **100**, 121113 (2012).
- <sup>9</sup>O. Buchnev, J. Y. Ou, M. Kaczmarek, N. I. Zheludev, and V. A. Fedotov, *Opt. Express* **21**, 1633 (2013).
- <sup>10</sup>M. Ren, B. Jia, J. Y. Ou, E. Plum, J. Zhang, K. F. MacDonald, A. E. Nikolaenko, J. Xu, M. Gu, and N. I. Zheludev, *Adv. Mater.* **23**, 5540 (2011).
- <sup>11</sup>G. A. Wurtz, R. Pollard, W. Hendren, G. P. Wiederrecht, D. J. Gosztola, V. A. Podolskiy, and A. V. Zayats, *Nat. Nanotechnol.* **6**, 107 (2011).
- <sup>12</sup>K. M. Dani, Z. Ku, P. C. Upadhyaya, R. P. Prasankumar, S. R. J. Brueck, and A. J. Taylor, *Nano Lett.* **9**, 3565 (2009).
- <sup>13</sup>A. E. Nikolaenko, F. D. Angelis, S. A. Boden, N. Papisimakis, P. Ashburn, E. D. Fabrizio, and N. I. Zheludev, *Phys. Rev. Lett.* **104**, 153902 (2010).
- <sup>14</sup>A. E. Nikolaenko, N. Papisimakis, E. Atmatzakis, Z. Luo, Z. X. Shen, F. De Angelis, S. A. Boden, E. Di Fabrizio, and N. I. Zheludev, *Appl. Phys. Lett.* **100**, 181109 (2012).
- <sup>15</sup>L. Ju, B. Geng, J. Horng, C. Girit, M. Martin, Z. Hao, H. A. Bechtel, X. Liang, A. Zettl, Y. R. Shen *et al.*, *Nat. Nanotechnol.* **6**, 630 (2011).
- <sup>16</sup>J. Zhang, K. F. MacDonald, and N. I. Zheludev, *Light Sci. Appl.* **1**, e18 (2012).
- <sup>17</sup>S. A. Mousavi, E. Plum, J. Shi, and N. I. Zheludev, *Appl. Phys. Lett.* **105**, 011906 (2014).
- <sup>18</sup>H.-T. Chen, W. J. Padilla, J. M. O. Zide, A. C. Gossard, A. J. Taylor, and R. D. Averitt, *Nature* **444**, 597 (2006).
- <sup>19</sup>W. J. Padilla, A. J. Taylor, C. Highstrete, M. Lee, and R. D. Averitt, *Phys. Rev. Lett.* **96**, 107401 (2006).
- <sup>20</sup>N. I. Zheludev and Y. S. Kivshar, *Nat. Mater.* **11**, 917 (2012).
- <sup>21</sup>M. Lapine, I. V. Shadrivov, D. A. Powell, and Y. S. Kivshar, *Nat. Mater.* **11**, 30 (2012).
- <sup>22</sup>H. Tao, A. C. Strikwerda, K. Fan, W. J. Padilla, X. Zhang, and R. D. Averitt, *Phys. Rev. Lett.* **103**, 147401 (2009).
- <sup>23</sup>D. Chicherin, S. Dudorov, D. Lioubtchenko, S. T. V. Ovchinnikov, and A. V. Raisanen, *Microw. Opt. Technol. Lett.* **48**, 2570 (2006).
- <sup>24</sup>W. M. Zhu, A. Q. Liu, X. M. Zhang, D. P. Tsai, T. Bourouina, J. H. Teng, T. Mei, G. Q. Lo, and D. L. Kwong, *Adv. Mater.* **23**, 1792 (2011).
- <sup>25</sup>Y. H. Fu, A. Q. Liu, W. M. Zhu, X. M. Zhang, D. P. Tsai, J. B. Zhang, T. Mei, J. F. Tao, H. C. Guo, X. H. Zhang *et al.*, *Adv. Funct. Mater.* **21**, 3589 (2011).
- <sup>26</sup>W. M. Zhu, A. Q. Liu, T. Bourouina, D. P. Tsai, J. H. Teng, X. Zhang, G. Q. Lo, D. L. Kwong, and N. Zheludev, *Nat. Commun.* **3**, 1274 (2012).
- <sup>27</sup>J. Y. Ou, E. Plum, L. Jiang, and N. I. Zheludev, *Nano Lett.* **11**, 2142 (2011).
- <sup>28</sup>J. Y. Ou, E. Plum, J. Zhang, and N. I. Zheludev, *Nat. Nanotechnol.* **8**, 252 (2013).
- <sup>29</sup>S. Prasanna and S. M. Spearing, *J. Microelectromech. Syst.* **16**, 248 (2007).